Optical Fiber Specklegram Sensor for Measurement of Force Myography Signals

Eric Fujiwara, Yu Tzu Wu, Murilo F. M. Santos, Egont A. Schenkel, and Carlos K. Suzuki

***Abstract*— The development of an optical fiber specklegram sensor for the assessment of force myography signals is reported. The device consists of microbending transducers attached to the user forearm by means of Velcro straps. The muscular stimuli generated in response to hand movements cause the fibers to be mechanically pressed by the deformer structures, resulting in light modulation. The optical signals are acquired and processed according to specklegram analysis, by computing the normalized intensity inner product of speckles for two reference postures. Finally, the average values are correlated to the fingers configurations by means of artificial neural networks. The system was evaluated for a set of 11 static gestures, making it possible to detect subtle variations in the spatial distribution of forces impressed by the forearm flexor and extensor muscles. Moreover, the technique was tested for different subjects, yielding an average accuracy of 89.9% on the estimation of fingers configurations, even with the utilization of a reduced number of transducers.**

***Index Terms*— Biomedical measurement, force measurement, optical fiber sensors, user interfaces.**

I. Introduction

THE monitoring of hand postures and movements plays an important role on the development of human-robot and human-computer interfaces. As the user inputs can be assessed in a more natural and intuitive way, hand tracking technologies become widely applied on the design of advanced systems, including robot-assisted medical and rehabilitation devices, teleoperation, and virtual reality environments, as well as for service and entertainment purposes [1], [2]. Nowadays, several invasive and non-invasive approaches for hand gesture detection have been proposed, including optical tracking, glove-based sensors, and surface electromyography (sEMG) analysis.

Optical tracking techniques usually perform the identification of hand configuration based on the frames acquired by static cameras, which can be accomplished with the aid of markers or by appearance methods [3]. Subsequently, the obtained data is processed according to the temporal and spatial contexts for the estimation of static or dynamic gestures [2], [4]. The utilization of computer vision systems provides a non-invasive analysis of the user hand, which can be implemented with inexpensive hardware [5], [6]. However, in addition to the limitations related to image acquisition rate and computational cost, optical tracking methods are affected by occlusion and influenced by the environmental illumination [7].

Another approach consists in the utilization of glove-based sensors for the direct measurement of hand joints angular displacements. These devices are commonly formed by a matrix of displacement sensing elements attached to a wearable substrate [1], making it possible to correlate the variations on transducers responses to the dynamic movements of fingers. Currently, different technologies have been applied on the development of glove-based devices, including resistive flexsensors [8], accelerometers combined with magnetic tracking [9], and optical fiber sensors [10]. Even though such wearable devices are not affected by fingers occlusion and can provide real-time response [7], this approach presents some drawbacks in terms of restriction to hand movements, influence of glove material, and relative high-cost [4], [5].

The assessment of hand postures can be also accomplished by sEMG, in which the electrical signals emitted from the forearm muscles are detected by means of electrodes placed over the user skin, and then processed to retrieve the movements and forces caused by multiple degrees-of-freedom of human hand [11], [12]. As the transducers are placed on the forearm, the sEMG provides the analysis of gestures in a non-invasive way. Moreover, in contrast to the abovementioned techniques, the electromyography allows to detect the intention of movements, which is suitable for the control of bionic prostheses by amputees [13], [14]. However, the implementation of this technique still presents limitations, since the acquisition of sEMG signals relies on the precise placement of the electrodes, and the transducers responses are affected by skin contact and humidity conditions [15].

In this sense, alternative approaches have been proposed for hand postures and forces tracking based on the monitoring of muscular activities, including the mechanomyography (MMG), sonomyography (SMG) and force myography (FMG). The MMG is based on the measurement of low-frequency vibrations generated by active skeletal muscle fibers [16]. The detection of such mechanical signals is usually performed by accelerometers or piezoelectric sensors placed

Manuscript received June 15, 2016; revised December 9, 2016; accepted December 9, 2016. Date of publication December 13, 2016; date of current version January 19, 2017. This work was supported in part by the Sao Paulo Research Foundation under Grant 2014/25080-0 and Grant 2015/01820-7, in part by UNICAMP/FAEPEX under Grant 519.292-0097/15, in part by CNPq, and in part by CAPES. The associate editor coordinating the review of this paper and approving it for publication was Prof. Tony Huang.

E. Fujiwara is with the Laboratory of Photonic Materials and Devices, State University of Campinas, 13083-970, Campinas, Brazil, and also with the Department of Integrated Systems, State University of Campinas, 13083-970, Campinas, Brazil (e-mail: fujiwara@fem.unicamp.br).

Y. T. Wu, M. F. M. Santos, and E. A. Schenkel are with the Laboratory of Photonic Materials and Devices, State University of Campinas, 13083-970 Campinas, Brazil.

C. K. Suzuki is with the Laboratory of Photonic Materials and Devices, State University of Campinas, 13083-970 Campinas, Brazil, and also with the Department of Materials and Manufacturing Engineering, State University of Campinas, 13083-970 Campinas, Brazil (e-mail: suzuki@fem.unicamp.br).

Digital Object Identifier 10.1109/JSEN.2016.2638831

over the skin surface [17]. In the case of the SMG, the deformation of musculoskeletal tissues due to hand movements are assessed by multidimensional ultrasound analysis, which can be accomplished by means of scanners [18]–[20]. Additionally, the utilization of optical tracking for muscles activation monitoring was also proposed in a recent research [21], in which the measurement of fingers movements was demonstrated.

Among these techniques, the FMG was proven to be a very promising method for the measurement of hand movements and forces, presenting advantages when compared to the sEMG in terms of performance, cost and feasibility [22]. In this approach, the forces exerted by forearm muscles during hand posture changes are acquired and then decoded in static or dynamic ways, being later correlated to the hand movements and forces [23]–[25]. Nowadays, several studies have been conducted to evaluate the utilization of FMG for multi-fingered bionic prosthesis control [23], [24], [26], as well as on the monitoring patients during rehabilitation procedures [27]. The FMG signals are usually detected by means of arrays of force sensing resistors (FSR) distributed over the forearm surface, which can be attached to the skin with the utilization of orthoses [26], garments [25] or straps [27]. Even though such devices provide an acceptable measurement of muscular stimulus, the FSR present drawbacks in terms of hysteresis and loss of sensitivity after repeated loading [28]. The assessment of applied pressures can be also carried out with the utilization of capacitive or piezoelectric sensors, but these sensors can present limitations concerning vulnerability to noise and resolution [29].

In this context, optical fiber sensors (OFS) have been widely adopted on the measurement of mechanical variables in healthcare and biomedical applications as alternatives to electrical approaches [30], [31], since they present inherent characteristics such as lightweight, flexibility, multiplexing and distributed sensing capabilities, remote operation, and immunity to electromagnetic interference [32], [33]. Examples of OFS-based systems include glove-based sensors [10], [34], [35], instrumented clothes for body movements detection [36], fiber embedded textiles for monitoring of heartbeat and respiration [37], [38], as well as invasive sensors for pressure measurements [32]. Moreover, preliminary studies regarding the utilization of OFS to retrieve FMG signals were also reported by the authors [39], [40], showing the feasibility of this technology on the tracking of hand postures and forces.

In this paper, the recent developments on the optical fiber specklegram sensor for the measurement of FMG signals are reported. The optomechanical transducers are attached to the user forearm by means of a modular structure, allowing the detection of the exerted forces. Finally, the actual hand configuration can be estimated from the acquired optical data by means of artificial neural networks (ANN) processing.

II. Optical Fiber Sensor

A. Fiber Specklegram Sensor

The FMG technique relies on the assessment of the forces produced by forearm muscles due to hand movements. Such mechanical stimuli can be detected by different OFS approaches, including intensity and spectral modulation schemes, for example, bending or fiber grating sensors, respectively [33]. In this research, the measurement of FMG signals was carried out by means of a specklegram-based technique, in which the mechanical disturbances applied to a multimode optical fiber cause variations on the output speckle pattern [42]. Fiber specklegram sensors present high sensitivity (since they take advantage of the modal phase information), multiplexing capability, and can be implemented with a simple interrogation scheme, being suitable for mechanical, thermal and chemical analyses [43], [44].

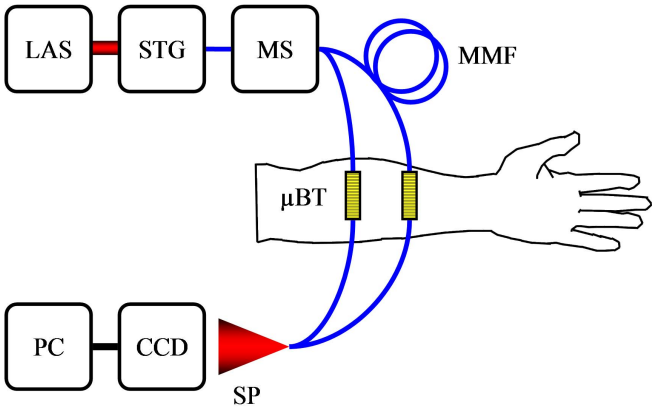

Fig. 1. Experimental setup of FMG sensor. LAS: laser source, STG: launching stage, MS: mode scrambler, MMF: multimode fiber, ìBT: microbending transducer, SP: output specklegram, CCD: camera, PC: computer.

In order to improve the sensor sensibility, the specklegram data can be processed by means of correlation techniques [42]. Given the light intensity $I(x,y)$ of a speckle field projected over a xy plane

$$I(x,y) = \sum_{m=0}^{M}\sum_{n=0}^{M} a_m a_n \exp[j(\phi_m - \phi_n)], \quad (1)$$

where M is the number of propagation modes, a and φ are the amplitudes and phase deviations, respectively, of the m-th and n-th modes, the normalized intensity inner product of specklegrams (*NIPC*) is calculated by

$$NIPC = \iint I_0 I dxdy / \left(\iint I_0^2 dxdy \iint I^2 dxdy\right)^{\frac{1}{2}}, \quad (2)$$

I_0 is the intensity for a reference fiber status [42].

B. Sensor Design

The optical fiber sensor system is shown in Fig. 1. The light emitted by a continuous HeNe laser source (663 nm) is launched into ~2 m length silica multimode fibers (plane-polished, 62.5 μm diameter core with polymer buffer) by means of a mechanical stage. Next, the waveguides are subjected to a mode scrambler in order to balance the modal power distribution, and then connected to the optomechanical transducers for assessment of FMG signals. Finally, the fibers end faces are carefully aligned by using a manual stage and the

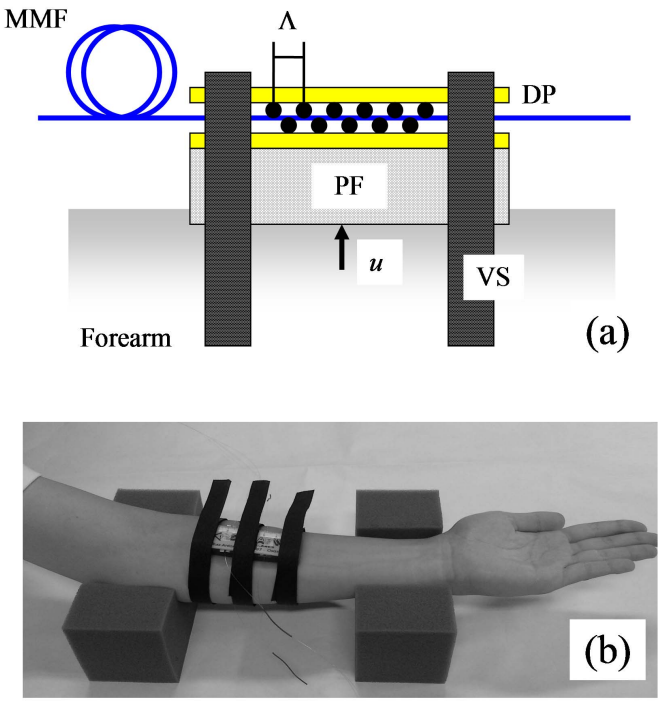

Fig. 2. (a) Schematic of optical fiber transducer. MMF: multimode fiber, DP: deformer plate, PF: polyurethane foam, VS: Velcro strap. A photograph of the sensing modules attached to the user forearm is shown in (b).

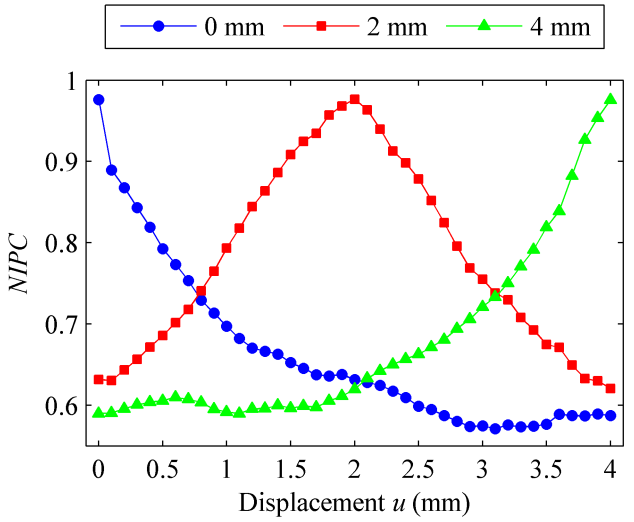

Fig. 3. Sensor response to linear displacements. The NIPC curves were calculated for different reference conditions, as indicated in the legend.

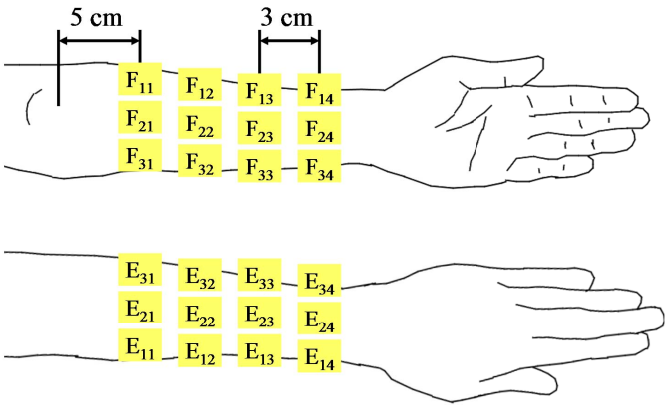

Fig. 4. Transducers positions on user forearm according to the supinated and pronated conditions. Positions F_{ij} and E_{ij} regard to the monitoring of flexors and extensor muscles, respectively.

output light spots are detected by a CCD camera (uEye, IDS, 1024 × 768 pixels, 15 fps), and then processed in a routine developed under MATLAB (Mathworks) environment.

The microbending transducers (Fig. 2) consist of a pair of deformer plates (0.5 mm diameter graphite rods attached to $20\times10\times1$ mm^3 polypropylene substrate) with a periodical structure ($\Lambda = 5$ mm) that interposes the waveguide and modulates the light in response to the muscular stimuli. As the transducers experience perpendicular displacements u, the microbendings cause energy coupling between the guided and the radiation modes [41], yielding both light attenuation and specklegram changes, which can be further correlated to the hand postures.

In order to monitor the forces generated by multiple muscles, a sensing module was designed by placing the transducer over an additional polypropylene plate provided with Velcro straps to adjust the device onto the subject forearm. The contact between the transducers and the skin is also intermediated by a 10 mm thickness polyurethane foam layer to improve the comfort to the user. It is worth noticing that multiple modules can be connected by the straps, making it possible to distribute the sensing probes along the forearm circumference.

The typical sensor static response for perpendicular displacements is presented in Fig. 3 [39]. The transducer was excited by a mechanical stage for $u = 0$ to $u = 4$ mm with 0.1 mm increment, by maintaining each condition for 2 s and considering the average of 2 upscale and 2 downscale experiments. The specklegrams were filtered by 2D discrete wavelet transform (Daubechies db4) for image denoising, followed by the calculation of *NIPC* for 3 reference statuses (0, 2, and 4 mm). As observed in Fig. 3, the *NIPC* decreases as the fiber status deviates from the reference one, reaching a saturation value after ~2 mm displacement, but the dynamic range can be extended by resetting I_0. Nevertheless, one may notice that the specklegram analysis presents fairly linear response for ≤ 2 mm displacement ranges, as well as reproducible behavior under controlled conditions.

III. Experimental Procedure

A. Measurement Protocol

The experiments were conducted on 4 healthy volunteers (3 males and 1 female, 27 ± 4 years old), with the subjects sitting in a comfortable position, considering the forearm extended in supinated condition and supported by the wrist and the elbow using semi-rigid foams in order to prevent application of external forces on the transducers, as well as to restrict the wrist flexion/extension and adduction/abduction movements.

Firstly, the microbending devices were tested for 24 positions over the forearm, as observed in Fig. 4, to monitor

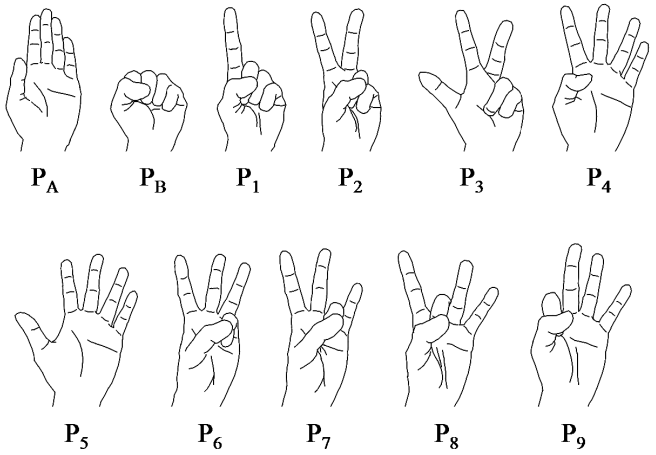

Fig. 5. Hand postures considered for the experiments. Postures PA and PB are used as references, whereas P_1 to P_9 are related to the numbers in manual alphabets.

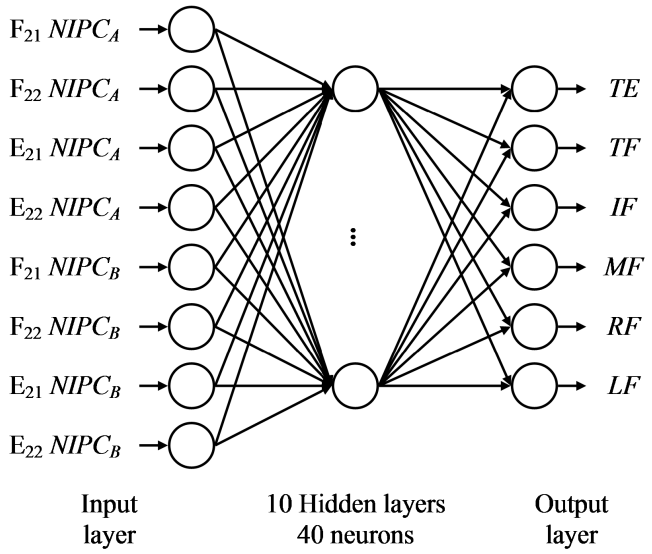

Fig. 6. Artificial neural network for hand posture estimation. The $NIPC_A$ and $NIPC_B$ values obtained from each transducer are correlated to the finger joints configurations by means of 10 hidden layers.

both flexors and extensors muscles. Each location is labeled according to the type of monitored muscle (F for flexor and E for extensor) and its absolute position on the forearm surface. The Velcro straps were tightly adjusted to prevent the transducers dislocations during the accomplishment of movements, and also to input a preload over the optical fiber, but without applying excessive forces. The experiments were carried out using 4 transducers per measurement (2 flexors and 2 extensors), but the locations of each probe were carefully registered to ensure the repeatability of the tests. After receiving a visual command, the subjects were requested to perform sequences of movements composed by sets of postures (Fig. 5) chosen in pseudo-random order, by keeping the hand configuration for 5 s per posture. Even though the subjects were oriented to reproduce the movements according to a strict protocol, eventual fluctuations on hand joints angles and grasping forces were expected, since the tests were conducted without the utilization of splints or hand motion limiting devices.

Next, the sensor performance on the identification of hand postures was evaluated by carrying out the experiments for all subjects. In order to minimize the number of measuring fibers and the computing costs during specklegrams processing, the tests were performed regarding 4 of 24 locations (F_{21}, F_{22}, E_{21}, and E_{22}), providing an averaged assessment of forearm muscles. The users were requested to perform sequences of gestures according to the abovementioned protocol, being the recorded values divided on training and test sets, and then subjected to data processing.

B. Data Processing

The acquired specklegrams were filtered by 2D wavelet transform followed by the *NIPC* calculation. The *NIPC* values were computed according to 2 reference postures (P_A and P_B, see Fig. 5), which were used for sensor calibration, resulting in 8 curves per set (4 transducers, 2 *NIPC* per device), where $NIPC_A$ and $NIPC_B$ denote the calculated values referenced to P_A and P_B, respectively. For the estimation of static hand configurations, the data were processed by ANN classifiers using MATLAB toolboxes [45]. The *NIPC* dataset were reduced by windowing the signals to exclude the frames related to posture changes, and then calculating the average value for each posture. The networks (Fig. 6) were designed according to the backpropagation architecture with tangent sigmoidal transfer functions, by addressing the 8 *NIPC* values to the input layer and setting the output layer as a 6 data structure representing the flexion/extension of each digit (0 for minimum and 1 for maximum angular displacement), also including 10 hidden layers of 40 neurons. For the network output, the hand configurations were coded as $\mathbf{y} = [\text{TE TF IF MF RF LF}]^{\text{T}}$, where TE is the thumb extension, TF is the thumb flexion, IF is the index finger flexion, MF is the middle flexion, RF is the ring flexion, and LF is the little flexion. For example, posture P_1 is expressed as $\mathbf{y}_1 = [0\ 1\ 0\ 1\ 1\ 1]^{\text{T}}$, indicating the extension of the index finger and the flexion of other digits. The networks were evaluated according to a 10-fold cross validation, being the training sessions conducted with scaled conjugated gradient backpropagation function, by choosing the mean squared error with regularization performance function with 0.5 performance parameter ratio and setting the training goal to 0.05. Finally, the system performance was evaluated by comparing the network output to the nominal values, and then computing the average results for all folds.

The ANN response was analyzed according to 3 parameters: (i) the ratio of postures correctly classified as positive per total number of positive cases (true positive ratio TP); (ii) the ratio of postures misclassified as positive per total number of negatives (false positive ratio FP); and (iii) the ratio of correct classifications (accuracy AC).

IV. Results and Discussion

A. Evaluation of Sensor Response

The variation of *NIPC* values during the accomplishment of a sequence of postures is shown in Fig. 7, regarding the

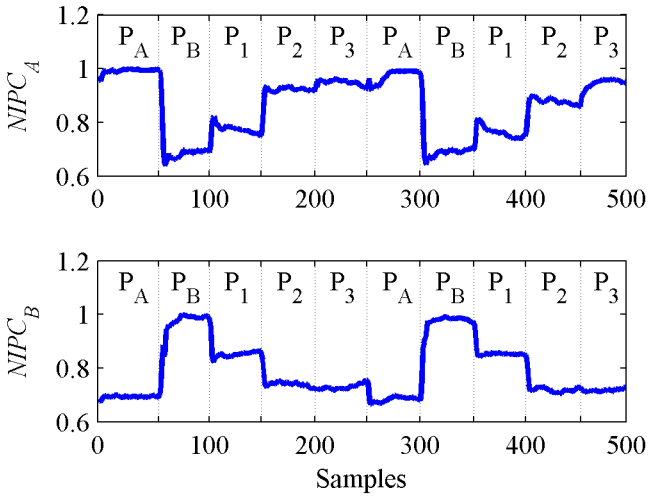

Fig. 7. Variation of $NIPC_A$ and $NIPC_B$ values as a function of hand postures (P_A, P_B, P_1, P_2, and P_3) for the transducer placed in position F_{21}.

transducers placed in position F_{21} for a single user. An analogous behavior can be observed in case of the other bending transducers and postures. The $NIPC_A$ and $NIPC_B$ assume maximum values when the hand is set to poses P_A and P_B, respectively, which correspond to the calibration conditions, whereas configurations P_1, P_2, and P_3 yield particular *NIPC* values that can present higher correlation to $NIPC_A$ or $NIPC_B$, depending on the hand joints configuration. The overall results considering all transducers locations (flexors and extensors) and postures are shown in Fig. 8 for $NIPC_A$, and Fig. 9 for $NIPC_B$. Each value represents the average of ~600 samples regarding one subject, corresponding to the hand in static conditions and by excluding the transitions between postures.

The *NIPC* distributions provide an optical correlation between the different postures based on the forces distributions generated by the forearm muscles. The monitored extrinsic muscles can produce mechanical stimuli due to the wrist and finger movements, as well as the forearm rotation. Since the wrist and the forearm were fixed during the experiments, the changes on *NIPC* values were expected to be caused mostly by the fingers flexion/extension and adduction/abduction.

Concerning the reference postures, P_A is characterized by the fingers in extended condition (open hand) without adduction or abduction of metacarpophalangeal joints, whereas P_B is defined by a clenched fist, with flexed fingers. Because of the maximum flexion of index, medium, ring, and little fingers, an intense activation of the flexor digitorum profundus (FDP) and superficiailis (FDS) muscles is expected in P_B, causing a high deviation between $NIPC_A$ and $NIPC_B$, especially considering the transducers placed in the forearm palmar aspect (F_{11} to F_{33}). Moreover, the flexion of thumb joint in P_B also contributes to the differentiation of the calibration postures, which is associated to the activation of the flexor pollicis longus (FPL) muscle, F_{11} to F_{24}. It is worth noticing that because the microbending transducers are set to monitor the forces on forearm surface, it is not possible to track the activation of individual muscles lied in different layers. Instead, the *NIPC* maps provide a representation of the average force distribution, which is related to the overall contribution of the assessed muscles. Regarding the dorsal aspect of the forearm, the fingers extension in PA implies on the activation of the extensor digitorum comunis (EDC) muscle, which can be assessed by transducers E_{11} to E_{33}. In addition, the thumb abduction and extension movements also result in variations on sensing elements E_{22} to E_{14} responses, due to the activation of abductor pollicis longus (APL) and extensor pollicis longus (EPL) muscles.

In case of postures P_1 to P_9, the *NIPC* values indicate an overall higher correlation to P_A rather than P_B. Particularly, configuration P_1 differs from P_B only in the index finger extension, yielding a significant correlation for $NIPC_B$, as observed in the FDP and FDS muscles. On the other hand, postures P_2, P_4 and P_5 gradually deviate (in this order) from PB and approach P_A, mostly because of the extension of fingers joints, resulting in pressure maps more similar to the open hand condition. The difference between postures P_4 and P_5 can be also detected by tracking the response of APL and EPL muscles. Using a similar analysis, the discrimination of P_2 and P_3 can be accomplished by monitoring the muscles related to the thumb movements. One may observe that the abduction/extension of thumb joints result in low correlation in both $NIPC_A$ and $NIPC_B$ maps regarding transducers E_{22} to E_{14}, since such movement was not covered by the calibration poses. Finally, postures P_6 to P_9 comprise the simultaneous flexion of a finger and the thumb. In practice, configurations P_6 and P_7 are fairly similar to P_2, presenting differences on the degree of flexion of the thumb, and on the extension of the little finger, related to the extensor digiti minimi (EDM) muscle, E_{21} to E_{33}. Analogously, the distinction between postures P_8 and P_9 are expected to be evidenced by the extensor indicis (EI) muscle, E_{21} to E_{24}, which is partially responsible for the index finger extension.

B. Posture Estimation

The estimation of fingers configurations by ANN for each subject are summarized in Table I, given the average of 10 folds. The overall results considering the mean of four subjects and fingers were FP = 10.4%, TP = 85.6%, and AC = 89.9%, showing that the fingers conditions were correctly obtained for most of cases. In order to elucidate the effect of the hand pose on the assessment of each digit, the network output were discriminated per posture in Fig. 10, presenting the comparison between the expected y values and the obtained ones, regarding the average of all subjects. The low true positive ratio (TP < 70%) for TE can be explained because the transducers were placed in locations less susceptible to the stimuli of APL muscle, as noted in postures P_3 and P_5, which could be solved by attaching an additional transducer in position E_{13}. On the other hand, higher false positive ratios (FP > 10%) were observed for TF, RF, and LF. The analysis of Fig. 10 indicates that most of LF misclassifications occurs for P_4 and P_7, whereas the errors related to RF are more evident for posture P_9. The differences among such configurations are detectable as subtle variations on the EDC, FDS, and FDP muscles mechanical

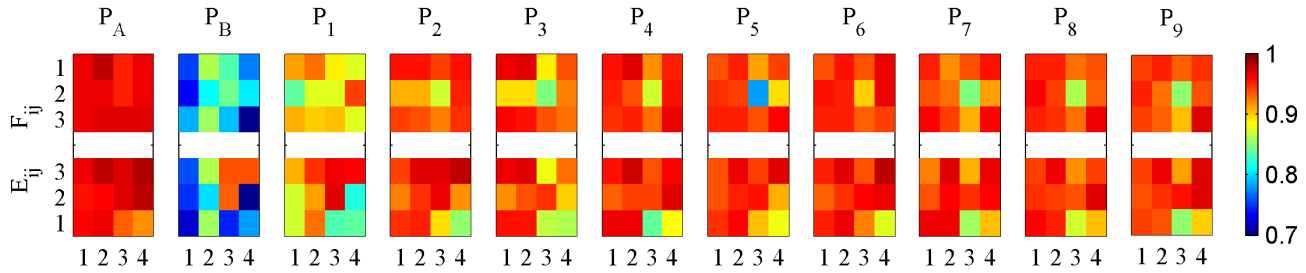

Fig. 8. Effect of transducers location on $NIPC_A$ values for different postures. Data for flexors (Fij) and extensors (Eij) are displayed in the same plot.

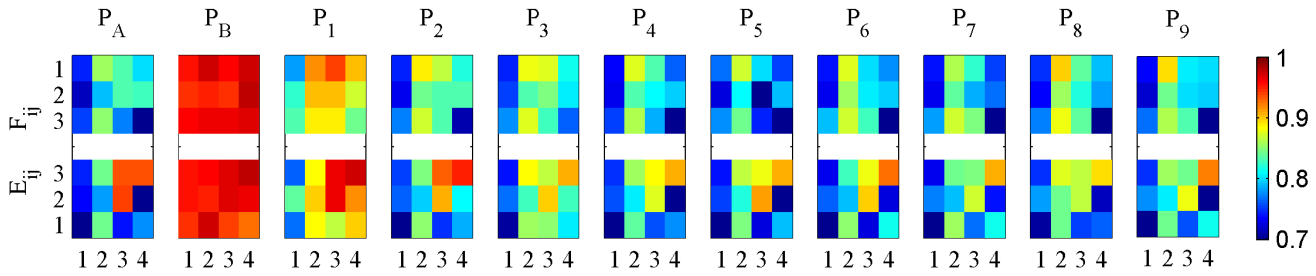

Fig. 9. Effect of transducers location on $NIPC_B$ values for different postures. Data for flexors (Fij) and extensors (Eij) are displayed in the same plot.

TABLE I

ANN PERFORMANCE ON THE ESTIMATION OF FINGERS CONFIGURATIONS FOR EACH SUBJECT. FP: FALSE POSITIVE RATIO; TP: TRUE POSITIVE RATIO; AC: ACCURACY

	Subjects				
	S1	S2	S3	S4	Mean
TE	FP = 5.6±3.1% TP = 61.9±24.9% AC = 90.3±3.2%	FP = 6.3±3.9% TP = 69.0±17.8% AC = 90.6±3.4%	FP = 6.6±7.7% TP = 76.2±21.2% AC = 91.2±6.2%	FP = 5.9±2.8% TP = 64.3±17.8% AC = 90.3±4.2%	FP = 6.1±4.5% TP = 67.9±20.2% AC = 90.6±4.2%
TF	FP = 23.3±10.0% TP = 92.2±5.2% AC = 86.9±3.8%	FP = 14.3±5.9% TP = 92.2±6.9% AC = 90.0±4.9%	FP = 22.3±8.0% TP = 91.7±6.7% AC = 86.9±5.0%	FP = 16.1±8.7% TP = 91.7±5.5% AC = 89.1±4.7%	FP = 19.0±8.8% TP = 91.9±5.8% AC = 88.2±4.5%
IF	FP = 2.5±2.0% TP = 85.7±8.2% AC = 94.2±2.9%	FP = 6.7±5.3% TP = 85.7±6.9% AC = 91.2±4.7%	FP = 2.5±3.1% TP = 91.2±8.2% AC = 95.7±2.7%	FP = 6.3±3.6% TP = 85.7±10.3% AC = 91.5±3.3%	FP = 4.5±4.0% TP = 87.1±8.4% AC = 93.2±3.8%
MF	FP = 10.1±7.3% TP = 90.2±6.1% AC = 90.0±4.0%	FP = 6.5±6.5% TP = 85.7±5.9% AC = 90.9±4.9%	FP = 3.2±3.2% TP = 97.3±3.3% AC = 97.0±2.1%	FP = 3.7±3.4% TP = 94.6±4.3% AC = 95.7±2.5%	FP = 5.9±5.8% TP = 92.0±6.6% AC = 93.4±4.5%
RF	FP = 14.3±8.3% TP = 83.1±5.1% AC = 84.5±5.2%	FP = 13.1±7.6% TP = 89.0±6.9% AC = ±87.8%2.7	FP = 9.7±5.6% TP = 92.9±9.4% AC = 91.5±4.6%	FP = 10.9±3.0% TP = 90.3±5.5% AC = 89.7±4.0%	FP = 12.0±6.3% TP = 88.8±7.5% AC = 88.4±4.8%
LF	FP = 14.3±7.6% TP = 89.0±7.4% AC = 87.2±4.4%	FP = 16.0±8.3% TP = 86.4±7.4% AC = 85.1±1.7%	FP = 14.9±7.6% TP = 84.4±6.9% AC = 84.8±2.9%	FP = 14.3±8.0% TP = 85.1±5.7% AC = 85.4±4.2%	FP = 14.9±7.5% TP = 86.2±6.7% AC = 85.6±3.4%

responses, caused by the extension of the index, medium, ring, and little fingers, therefore the individual identification of finger movements was probably hindered because the activation of these digits is bounded to the same muscles. In particular, the errors related to LF could be ameliorated by monitoring the EDM activity from position E_{33}, yielding a more sensible detection. Finally, the misclassifications related to TF were mostly observed for P_3 probably due to the low sensitivity during the monitoring of APL muscle, causing the network to misidentify P_3 as P_2.

Furthermore, the results were also expected to be affected by variations on performed postures and applied forces, since the experiments were carried out without using splints or molds to limit the joints displacements. The application of excessive forces during fingers flexion also leads to the increase of load over the microbending transducers, yielding deviations in the specklegrams, which result in different *NIPC* values, and consequently the misclassification of that posture. In this sense, the sensor performance could be improved by conducting a more intensive calibration procedure to increase the network generalization capability, or by utilizing additional transducers, providing data from supplementary groups of muscles and reducing the classification ambiguities. On the other hand, in the case of the presented system, the utilization

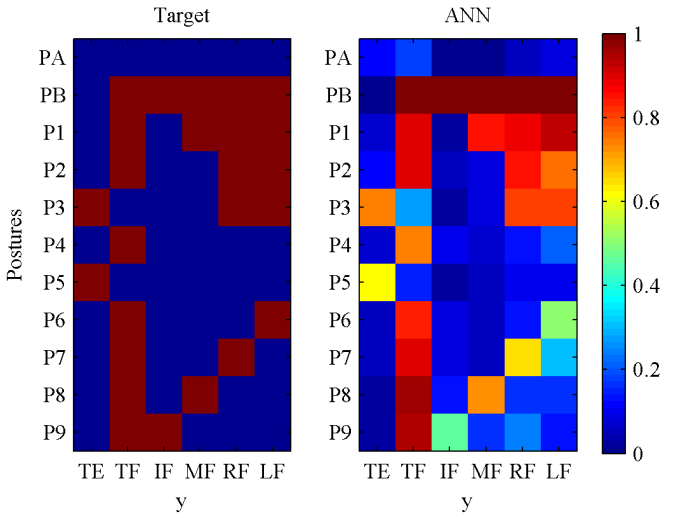

Fig. 10. Comparison of expected fingers configurations y and ANN results for each posture, regarding the average of all subjects.

of extra transducers could be avoided by computing the *NIPC* for additional reference poses. According to Fig. 8 and Fig. 9, both $NIPC_A$ and $NIPC_B$ tend to assume minimum values as the current posture deviates from the reference one. However, as the *NIPC* value is reduced, the specklegram sensor sensibility for mechanical displacements also decreases, making the system less responsive for variations in hand configuration. Therefore, changing the reference speckle pattern generates a different *NIPC* dataset, which could improve the classification performance for a particular group of postures. For example, calculating the *NIPC* in relation to P_9 would result in a better discrimination of P_7, P_8, and P_9. Finally, it is worth noticing that the results were conducted by calculating the average *NIPC* values for static postures. Conversely, making use of the dynamic data, as usually performed in sEMG-based systems [12], could increase the sensor response, as the ANN will carry out the classification also based on temporal features (including the postures transitions) of *NIPC* data. Nevertheless, depending on the complexity of the involved hand poses and the available hardware capabilities, the results provided by static approach can be sufficient for the required application.

V. Conclusion

The application of the optical fiber sensor for FMG signals analysis with further estimation of hand postures was demonstrated, yielding average accuracy of 89.9%. In contrast to the current technologies, the assessment of the forces impressed by forearm muscles was carried out with a reduced number of transducers, and the optical signals were processed based on assessment of speckle correlation.

For practical aspects, the hardware for light emission and signals interrogation can be integrated and miniaturized in a separated unit or embedded system, with the force transducers connected by fiber cables for remote assessment of the user forearm, which would be convenient for consumer applications. Furthermore, the sensor output can be utilized for patients monitoring or bionic manipulators control.

Even though the system provided poorer response for retrieving the flexion/extension of individual fingers, the results could be enhanced by increasing the number of measuring points or by taking advantage on the temporal characteristics of optical signals. Such improvements are currently under investigation by the authors and will be presented in further works, as well as the application of the proposed technology in the fields of human-robot interfaces and rehabilitation systems.

References

[1] L. Dipietro, A. M. Sabatini, and P. Dario, "A survey of glove-based systems and their applications," *IEEE Trans. Syst., Man, Cybern. C, Appl. Rev.*, vol. 38, no. 4, pp. 461–482, Jul. 2008.

[2] S. Mitra and T. Acharya, "Gesture recognition: A survey," *IEEE Trans. Syst., Man, Cybern. C, Appl. Rev.*, vol. 37, no. 3, pp. 311–324, May 2007.

[3] A. Jaimes and N. Sebe, "Multimodal human–computer interaction: A survey," *Comput. Vis. Image Understand.*, vol. 108, nos. 1–2, pp. 116–134, Oct./Nov. 2007.

[4] V. I. Pavlovic, R. Sharma, and T. S. Huang, "Visual interpretation of hand gestures for human-computer interaction: A review," *IEEE Trans. Pattern Anal. Mach. Intell.*, vol. 19, no. 7, pp. 677–695, Jul. 1997.

[5] A. Erol, G. Bebi, M. Nicolescu, R. D. Boyle, and X. Twombly, "Vision-based hand pose estimation: A review," *Comput. Vis Image Understand.*, vol. 108, nos. 1–2, pp. 52–73, Oct./Nov. 2007.

[6] Z. Ren, J. Yuan, J. Meng, and Z. Zhang, "Robust part-based hand gesture recognition using kinetic sensor," *IEEE Trans. Multimedia*, vol. 15, no. 5, pp. 1110–1120, Aug. 2013.

[7] D. J. Sturman and D. Zeltzer, "A survey of glove-based input," *IEEE Comput. Graph.*, vol. 14, no. 1, pp. 30–39, Jan. 1994.

[8] G. Saggio, "A novel array of flex sensors for a goniometric glove," *Sens. Actuators A, Phys.*, vol. 205, pp. 119–125, Jan. 2014.

[9] H. G. Kortier, V. I. Sluiter, D. Roetenberg, and P. H. Veltink, "Assessment of hand kinematics using inertial and magnetic sensors," *J. Neuroeng. Rehabil.*, vol. 11, pp. 70:1–7:14, Apr. 2014.

[10] E. Fujiwara, M. F. M. Santos, and C. K. Suzuki, "Flexible optical fiber bending transducer for application in glove-based sensors," *IEEE Sensors J.*, vol. 14, no. 10, pp. 3631–3636, Oct. 2014.

[11] C. Fleischer and G. Hommel, "A human–exoskeleton interface utilizing electromyography," *IEEE Trans. Robot.*, vol. 24, no. 2, pp. 872–882, Aug. 2008.

[12] C. Disselhorst-Klug, T. Schmitz-Rode, and G. Rau, "Surface electromyography and muscle force: Limits in sEMG-force relationship and new approaches for applications," *Clin. Biomech.*, vol. 24, no. 3, pp. 225–235, Aug. 2009.

[13] C. Castellini, E. Gruppioni, A. Davalli, and G. Sandini, "Fine detection of grasp force and posture by amputees via surface electromyography," *J. Physiol. Paris*, vol. 103, nos. 3–5, pp. 255–262, May/Sep. 2009.

[14] R. G. E. Clement, K. E. Bugler, and C. W. Oliver, "Bionic prosthetic hands: A review of present technology and future aspirations," *Surgeon*, vol. 9, no. 6, pp. 336–340, Dec. 2011.

[15] P. Heo, G. M. Gu, S.-J. Lee, K. Rhee, and J. Kim, "Current hand exoskeleton technologies for rehabilitation and assistive engineering," *Int. J. Precis. Eng. Manuf.*, vol. 13, no. 5, pp. 807–824, May 2012.

[16] T. W. Beck *et al.*, "Mechanomyographic amplitude and frequency responses during dynamic muscle actions: A comprehensive review," *Biomed. Eng. Online*, vol. 4, pp. 67:1–67:27, Dec. 2005.

[17] N. Alves and T. Chau, "Uncovering patterns of forearm muscle activity using multi-channel mechanomyography," *J. Electromyograph. Kinesiol.*, vol. 20, no. 5, pp. 777–786, Oct. 2010.

[18] Y. P. Zheng, M. M. F. Chan, J. Shi, X. Chen, and Q. H. Huang, "Sonomyography: Monitoring morphological changes of the forearm muscles in actions with the feasibility for the control of powered prosthesis," *Med. Eng. Phys.*, vol. 28, no. 5, pp. 405–415, Jun. 2006.

[19] J.-Y. Guo, Y.-P. Zheng, L. P. J. Kenney, A. Bowen, D. Howard, and J. J. Chanderle, "A comparative evaluation of sonomyography, electromyography, force, and wrist angle in a discrete tracking task," *Ultrasound Med. Biol.*, vol. 37, no. 6, pp. 884–891, Jun. 2011.

[20] D. S. González and C. Catellini, "A realistic implementation of ultrasound imaging as a human-machine interface for upper-limb amputees," *Front. Neurorobot.*, vol. 7, pp. 17:1–17:11, Oct. 2013.

[21] C. Nissler, N. Mouriki, C. Castellini, V. Belagiannis, and N. Navab, "OMG: Introducing optical myography as a new human machine interface for hand amputees," in *Proc. ICORR*, Aug. 2015, pp. 937–942.

[22] V. Ravindra and C. Catellini, "A comparative analysis of three non-invasive human-machine interfaces for the disabled," *Front. Neurorobot.*, vol. 8, pp. 24:1–24:10, Oct. 2014.

[23] R. L. Abboudi, C. A. Glass, N. A. Newby, J. A. Flint, and W. Craelius, "A biomimetic controller for a multifinger prosthesis," *IEEE Trans. Rehabil. Eng.*, vol. 7, no. 2, pp. 121–129, Jun. 1999.

[24] W. Craelius, "The bionic man: Restoring mobility," *Science*, vol. 295, no. 5557, pp. 1018–1021, Feb. 2002.

[25] M. Wininger, N.-H. Kim, and W. Craelius, "Pressure signature of forearm as predictor of grip force," *J. Rehabil. Res. Devices*, vol. 45, no. 6, pp. 883–892, Jul. 2008.

[26] N. Carbonaro *et al.*, "An innovative multisensor controlled prosthetic hand," in *Proc. MEDICON*, 2013, pp. 93–96.

[27] Z. G. Xiao and C. Menon, "Towards the development of a wearable feedback system for monitoring the activities of the upper-extremities," *J. Neuroeng. Rehabil.*, vol. 11, pp. 2:1–2:13, Jan. 2014.

[28] J. G. Dabling, A. Filatov, and J. W. Wheeler, "Static and cyclic performance evaluation of sensors in human interface pressure measurement," in *Proc. EMBC*, Sep. 2012, pp. 162–165.

[29] M. I. Tiwana, S. J. Redmond, and N. H. Lovell, "A review of tactile sensing technologies with applications in biomedical engineering," *Sens. Actuators A, Phys.*, vol. 179, pp. 17–31, Jun. 2012.

[30] V. Mishra, N. Singh, U. Tiwari, and P. Kapur, "Fiber grating sensors in medicine: Current and emerging applications," *Sens. Actuators A, Phys.*, vol. 167, no. 2, pp. 279–290, Jun. 2011.

[31] A. G. Mignani and F. Baldini, "Fibre-optic sensors in healthcare," *Phys. Med. Biol.*, vol. 42, no. 5, pp. 967–979, May 1997.

[32] P. Roriz, O. Frazão, A. B. Lobo-Ribeiro, J. L. Santos, and J. A. Simões, "Review of fiber-optic pressure sensors for biomedical and biomechanical applications," *J. Biomed. Opt.*, vol. 18, no. 5, pp. 050903:1–050903:18, May 2013.

[33] B. Culshaw, "Optical fiber sensor technologies: Opportunities and—Perhaps-pitfalls," *J. Lightw. Technol.*, vol. 22, no. 1, pp. 39–50, Jan. 1, 2014.

[34] M. Nishiyama and K. Watanabe, "Wearable sensing glove with embedded hetero-core fiber-optic nerves for unconstrained hand motion capture," *IEEE Trans. Instrum. Meas.*, vol. 58, no. 12, pp. 3995–4000, Dec. 2009.

[35] A. F. da Silva, A. F. Gonçalves, P. M. Mendes, and J. H. Correia, "FBG sensing glove for monitoring hand posture," *IEEE Sensors J.*, vol. 11, no. 10, pp. 2442–2448, Oct. 2011.

[36] Y. Koyama, M. Nishiyama, and K. Watanabe, "A motion monitor using hetero-core optical fiber sensors sewed in sportswear to trace trunk motion," *IEEE Trans. Instrum. Meas.*, vol. 62, no. 4, pp. 828–836, Apr. 2013.

[37] A. Grillet *et al.*, "Optical fiber sensors embedded into medical textiles for healthcare monitoring," *IEEE Sensors J.*, vol. 8, no. 7, pp. 1215–1222, Jul. 2008.

[38] A. F. Silva, J. P. Carmo, P. M. Mendes, and J. H. Correia, "Simultaneous cardiac and respiratory frequency measurement based on a single fiber Bragg grating sensor," *Meas. Sci. Technol.*, vol. 22, no. 7, pp. 075801:1–075801:5, Jun. 2011.

[39] E. Fujiwara, Y. T. Wu, M. F. M. Santos, E. A. Schenkel, and C. K. Suzuki, "Development of an optical fiber FMG sensor for the assessment of hand movements and forces," in *Proc. ICM*, Mar. 2015, pp. 176–181.

[40] E. Fujiwara, Y. T. Wu, M. F. M. Santos, E. A. Schenkel, and C. K. Suzuki, "Identification of hand postures by force myography by using an optical fiber specklegram sensor," *Proc. SPIE*, vol. 9634, p. 96343Z, Sep. 2015, doi: 10.1117/12.2194605.

[41] J. W. Berthold, "Historical review of microbend fiber-optic sensors," *J. Lightw. Technol.*, vol. 13, no. 7, pp. 1193–1199, Jul. 1995.

[42] F. T. S. Wu, M. Wen, S. Yin, and C.-M. Uang, "Submicrometer displacement sensing using inner-product multimode fiber speckle fields," *Appl. Opt.*, vol. 32, no. 25, pp. 4685–4689, Sep. 1993.

[43] L. Rodriguez-Cobo, M. Lomer, and J. M. Lopez-Higuera, "Fiber specklegram-multiplexed sensor," *J. Lightw. Technol.*, vol. 33, no. 12, pp. 2591–2597, Jun. 15, 2015.

[44] E. Fujiwara, Y. T. Wu, and C. K. Suzuki, "Vibration-based specklegram fiber sensor for measurement of properties of liquids," *Opt. Laser Eng.*, vol. 50, no. 12, pp. 1726–1730, Dec. 2012.

[45] H. Demuth and M. Beale, *Neural Network Toolbox for Use With Matlab—User's Guide*. Natick, MA, USA: Mathworks, 2000.

Eric Fujiwara was born in Sao Paulo, Brazil. He received the B.S. degree in control and automation engineering, and the M.S. and Ph.D. degrees in mechanical engineering from the State University of Campinas (Unicamp), Campinas, Brazil, in 2008, 2009, and 2012, respectively.

From 2004 to 2013, he was a Research Assistant with the Laboratory of Photonic Materials and Devices, Unicamp. Since 2014, he has been an Assistant Professor with the Faculty of Mechanical Engineering, Unicamp. He is an author of more than 40 journal and conference papers, and seven inventions. His research interest includes the development of optical fiber sensor systems for applications in human-robot interaction, measurement of physical and chemical parameters using fiber sensors, and fabrication and application of silica nanoparticles, silica glasses, and specialty optical fibers.

Yu Tzu Wu was born in Taipei, Taiwan. She received the B.S. degree in control and automation engineering from the State University of Campinas (Unicamp), Campinas, Brazil, in 2015.

Since 2012, she has been with the Laboratory of Photonic Materials and Devices, Unicamp. Her research interest includes the development of mechatronics systems for applications in human-robot interaction and image processing.

Murilo F. M. Santos was born in Rio Claro, Brazil. He received the B.S. and M.S. degrees in mechanical engineering from the State University of Campinas (Unicamp), Campinas, Brazil, in 2012 and 2014, respectively.

Since 2009, he has been with the Laboratory of Photonic Materials and Devices, Unicamp. His research interests include the development of SiO2-based photonic materials.

Egont A. Schenkel was born in Campinas, Brazil. He received the B.S. degree in physics and the M.S. degree in mechanical engineering from the State University of Campinas (Unicamp), Campinas, in 2010 and 2015, respectively.

Since 2013, he has been with the Laboratory of Photonic Materials and Devices, Unicamp. His research interests include the development of SiO2-based photonic materials.

Carlos K. Suzuki was born in Sao Paulo, Brazil. He received the B.S. degree in physics from the University of Sao Paulo, Sao Paulo, in 1969, the M.S. degree in physics from the State University of Campinas (Unicamp), Campinas, Brazil, in 1974, and the Ph.D. degree in applied physics engineering from the University of Tokyo, Tokyo, Japan, in 1981.

He joined the Optical Fiber Project of Telebras, Unicamp, in 1982, where he was involved in the development of optical fiber preforms. From 1984 to 1990, he coordinated international cooperation projects of JICA and METI/ITIT, Unicamp, where he was developing highly perfect synthetic quartz and high-purity silica glass. From 1990 to 1993, he was a Research Fellow with the SPring-8 Laboratory, Harima, Japan. Since 1994, he has been a Professor of Materials Engineering in the area of optical materials, optical fiber sensors, and nanotechnology with Unicamp. He has authored more than 160 journal and conference papers, and holds over 15 patents.

Dr. Suzuki is a member of the Brazilian Society of Materials Research.